Mechanics of Advanced Composite Structures 9 (2022) 1–10

Semnan University

Mechanics of Advanced Composite Structures

journal homepage: http://MACS.journals.semnan.ac.ir

Analysis of SH-waves Propagating in Multiferroic Structure with Interfacial Imperfection

A. Singhal[a*], J. Baroi[a], M. Sultana[b], R. Baby[a]

[a] *School of Sciences, Christ University, Ghaziabad, 201003, India*
[b] *Department of Finance and Economics, Jagdish Sheth School of Management, Bangalore, India*

KEYWORDS

Mechanical vibrations
Analytical modeling
PM ($CoFe_2O_4$) material
Reinforced material

ABSTRACT

This article presents the study of wave mechanics in a multiferroic structure having imperfection in the structure's interface. This article reflects the study of shear horizontal (SH) wave propagation in a layered cylindrical structure consisting of thin layers of different materials (reinforced material and piezomagnetic material) with an imperfect interface. The interface considered between both materials is mechanically imperfect. Dispersion relations are achieved analytically. Distinct graphs are drawn (numerically) to exhibit the influence of parameters like rotation, initial stress, and mechanically imperfect parameters on phase velocity. Numerical results are drawn analytically and explained for each affecting distinct parameters for materials and interface. Parametric results on the phase velocities yield a significant conclusion of which some are: (a) Performance of Piezo with reinforcement material have an influential impact on wave velocity. (b) The mechanical imperfection affects the significantly on wave velocity (c) The Reinforcement/PM stiffening can monotonically up the velocity of phase velocity.

1. Introduction

Piezomagnetic material is the typical material that came in the category of multiferroic composites. Together with piezoelectric material, they possess the magneto-electric effect (ME effect). Smart materials are extensively helpful in the manufacturing of actuators, rotating sensors, acoustic devices, control sensors, transducers, etc. The surface acoustic wave (SAW) devices work on the basics of wave propagation in an elastic body of free surfaces where the distribution is localized near the surface area. Hence, the surface wave transmission smart composite materials have vital importance [1,2]. In current years, numbers of research papers are available, which depicts that many efforts have been taken to determine the magneto-electric effect in the Piezo composites [3-7] in the absence of rotation. Researchers studied out the elastic surface waves propagation in smart composite structures [8,9], some in MEE bi-materials structures with coupled interfacial imperfections [10-12], and through multilayered composite structures [13,14].

Nowadays many frameworks (e.g., Sensors, smart screens, transducers, etc.) consist of at least two constituents for better stability. Moreover, the combination of materials (composite materials structures) has better stability, efficiency, and performance with respect to those constituents' materials that work solely. The inclusion of piezomagnetic ceramic, in any edifice can assist to help for controlling structural functioning by the magnetically induced strain fields, also employ strain induced magnetic field as a feedback driver. Now, several studies on transverse seismic wave characteristics in piezo-composite structure materials have been published recently [15-18]. Dispersion characteristics of a dispersive wave become important to exhibit the design of the signal filtering for surface acoustics waves devices. The group of Wu et al. [19] studied the surface influence of the SH wave regarding their surface spectra in multiferroic nanoplates. Moreover, the two researchers Sun and Cheng [20] depicted that by altering the framework or by the addition of some conducting material metallic film with piezo medium, then the desired dispersion is achieved.

* Corresponding author. Tel.: +918374479212
E-mail address: ism.abhinav@gmail.com

DOI: 10.22075/macs.2021.20627.1266
Received 2020-06-15; Received in revised form 2021-09-05; Accepted 2021-12-13.

In the present study, the considered structure is a piezomagnetic material cylinder enclosed by the self-reinforced material with a mechanically imperfect interface. Self-reinforced materials are developed by the composition of fiber and matrix of the same material under specific temperature and pressure. Practically the self-reinforced material is stiffer, stronger, and discontinuous in contrast to the further anisotropic materials. This material has huge applications due to its extra deformation capacity. Whenever self-reinforced anisotropic materials exhibit electro-mechanical properties, these materials are applicable in the manufacturing of magnetic actuators, artificial muscles, etc. [21-24]. Verma and Rana [25] studied the influence of rotation on cylindrical structure tubes reinforced by fibers along a helical path. Moreover, Mahanty et al. [26] also studied the dispersion characteristics of shear waves in layered cylindrical fiber-reinforced media.

Two types of interfaces exist i.e., perfect interface and imperfect interface. Mostly, the composite material structures, the considered interface between the distinct materials is not perfect. The causes of imperfection may be microdefects, corrosion, aging of glue used between interfaces, or any accumulated damage. Such type of imperfection influences the transference behavior of considered waves remarkably. Wang et al. [27] and Fang et al. [28] displayed clearly the effect of the imperfection of the interface on the wave propagation through the materials. Moreover, some researchers used a linear spring model of the interfacial imperfection to exhibit their influence on wave propagation through different channels [29-31]. Therefore, the consideration of interfacial imperfection in the current research article brings it near to the real-world scenario. So, this research paper fills the gap between previous works done by the researchers which were only limited to a plain interface, but this paper introduced the concept of mechanical imperfect interface with different materials (reinforced material and piezomagnetic material).

However, sometimes during the different fabrication stages and manufacturing process, somehow there is a presence of initial stress in the medium. Therefore, it is necessary to consider the presence of initial stress in piezomagnetic material or structure. [32-34] consider the initial stress to make a better representation of their results without any error in the piezo-composite structures. Necessary discussion on composite structures using wave transmission through smart material under some mechanical stresses is carried out in [35-45].

This paper is going to exhibit clearly the SH wave vibrations transference in an initially stressed piezomagnetic cylinder coated with a thin layer of self-reinforced material and the interface considered between both materials is mechanical damage. The effects of a mechanically damaged imperfect interface, thickness ratio, reinforcement, initial stress, and piezomagnetic parameters are extensively shown on the phase velocity of SH waves. The outcomes of the present work will provide references for designing engineering PM composites.

2. Formulation of the problem and Equations

The present study describes a central cylindrical model, which is comprised of two distinct materials i.e., piezomagnetic and self-reinforced material as shown in figure 1. It consists of a pre-stressed piezomagnetic cylinder and a traction free concentric self-reinforced material-covering layer. The outer radius is r_{SR} and inner radius r_{pm} of the cylinder. The cylindrical coordinate system $r, \theta, z$is considered.

2.1. Wave analysis for PM Medium and equations

For SH wave propagation in pre-stressed PM composites, an anti-plane shear motion, displacement, and magnetic potential in the plane are given as Sun et al. [10].

$$u = v = 0, w = w(r, \theta, t), \psi = \psi(r, \theta, t) \tag{1}$$

where u, v, w represents mechanical displacement, ψ represents magnetic potential, respectively.

$$\begin{aligned} &\left(G_{pm} + P_1\right)\nabla^2 u_{pm} + h_{15}\nabla^2\psi_{pm} = \\ &\rho_{pm}\left(\partial u_{pm}/\partial t^2\right) \\ &h_{15}\nabla^2 u_{pm} - \mu_{pm}\nabla^2\psi_{pm} = 0. \end{aligned} \tag{2}$$

The consecutive equations for the PM materials can be expressed as Sun et al.

$$\begin{aligned} \sigma_{rz}^{pm} &= G_{pm}\left(u_{pm}\right)_{,r} + h_{15}\left(\phi_{pm}\right)_{,r}, \\ \sigma_{\theta z}^{pm} &= \frac{1}{r}\left(G_{pm}\left(u_{pm}\right)_{,\theta} + h_{15}\left(\phi_{pe}\right)_{,\theta}\right), \\ B_r^{pm} &= h_{15}\left(u_{pm}\right)_{,r} - \mu_{pm}\left(\psi_{pm}\right)_{,r}, \\ B_\theta^{pm} &= \frac{1}{r}\left(h_{15}\left(u_{pm}\right)_{,\theta} - \mu_{pm}\left(\psi_{pm}\right)_{,\theta}\right), \end{aligned} \tag{3}$$

In Eq. (2) and (3), G_{pm} and h_{15}represents the elastic, and PM coefficients, respectively; μ_{pm} denotes magnetic permeability ρ_{pm} and P_1 symbolizes the mass density and initial stress of the Piezo-material layer. The subscripts and superscript "pm" represent the quantities for the PM cylinder and the superimposed dot symbolizes the time derivative.

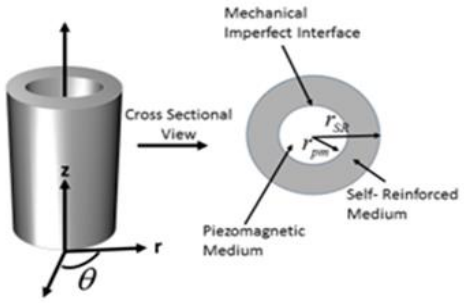

Fig. 1. A schematic of stratified multiferroic structure

$\nabla^2 = \frac{\partial^2}{\partial r^2} + \frac{1}{r}\frac{\partial}{\partial r} + \frac{1}{r^2}\frac{\partial^2}{\partial \theta^2}$ is Laplacian operator in polar coordinates.

In Eq. (4) and (5), σ_{iz}, and $B_i (i = r, \theta)$ represents anti-plane stress and magnetic induction respectively. The subscript comma represents a partial derivative with respect to coordinates.

Now we assume new auxiliary functions $\bar{\psi}_{pm}$ in the following form

$$\bar{\psi}_{pm} = \psi_{pm} - \frac{h_{15}}{\mu_{11}} u_{pm} \tag{4}$$

Introducing Eq. (4) into Eqs. (2), we get the decoupled equations

$$(\overline{G}_{pm} + P_1)\nabla^2 u_{pm} - \rho_{pm}\frac{\partial^2 u_{pm}}{\partial t^2} = 0, \nabla^2 \bar{\psi}_{pm} = 0, \tag{5}$$

where $\overline{G}_{pm} = G_{pm} + \frac{(h_{15})^2}{\mu_{11}}$

Consider the solution of Eq. (4) as

$$\begin{aligned} u_{pm} &= U_{pm}(r) e^{i(n\theta - \omega t)}, \\ \overline{\psi}_{pm} &= \Psi_{pm}(r) e^{i(n\theta - \omega t)} \end{aligned} \tag{6}$$

where $U_{pm}(r), \Psi_{pm}(r)$ are the unknown functions. n and ω represent wave number and angular frequency respectively. Substituting Eq. (6) into Eq. (5), yields the general solution in the following form.

$$\begin{aligned} u_{pm}(r) &= [A_1 J_n(\lambda_1 r) +] e^{i(n\theta - \omega t)}, \\ \overline{\psi}_{pm}(r) &= \left(A_2 r^n + A_1 \frac{h_{15}}{\mu_{11}} J_n(\lambda_1 r)\right) e^{i(n\theta - \omega t)} \end{aligned} \tag{7}$$

where $\lambda_1 = \frac{\omega \rho_{pm}}{\overline{G}_{pm} + P_1}$ and A_1, A_2 are unknown constants. J_n is Bessel functions of nth order of the first kind respectively.

2.2. Wave analysis for Self-Reinforced Medium and equations

Let u_i, v_i and w_i presents the mechanical displacement in r, θ, and z directions respectively. On the assumption that for propagating SH wave θ direction the composite is under axial shear deformation, we consider

$$u_i = v_i = 0, w_i = w_i(r, \theta, t), \frac{\partial}{\partial z} \equiv 0 \tag{8}$$

The fundamental governing equation for the self-reinforced material is

$$\frac{\partial T_{rz}^{SR}}{\partial r} + \frac{1}{r}\frac{\partial T_{\theta z}^{SR}}{\partial \theta} + \frac{\partial T_{zz}^{SR}}{\partial z} + \frac{T_{rz}^{SR}}{r} = \rho^{SR}\frac{\partial^2 w_{SR}}{\partial t^2} \tag{9}$$

where $T_{ij}^{SR}, \rho^{SR}, w_{SR}$ symbolizes the stress, density, and mechanical displacement along z direction, respectively.

The constitutive relations with directions of reinforcement along with unit vector $\vec{a}$ is given by [22].

$$\begin{aligned} T_{lm}^{SR} &= \gamma e_{ii}\delta_{lm} + 2\mu T e_{lm} \\ &+\alpha\left(a_i a_j e_{ij}\delta_{lm} + e_{ii} a_l a_m\right) \\ &+2(\mu_L - \mu_T)(a_l a_i e_{im} + a_m a_i e_{im}) \\ &+\beta a_i a_j e_{ij} a_l a_m, (i, j, l, m = r, \theta, z) \end{aligned} \tag{10}$$

Now, in the present work assumption of reinforcement direction is $\vec{a} = (0,1,0)$ From Eq. (10).

$$\begin{aligned} T_{rz}^{SR} &= 2\mu_T e_{rz}, \quad T_{\theta z}^{SR} = 2\mu_L e_{\theta z}, \\ T_{zz}^{SR} &= \gamma e_{rr} + (\gamma + \alpha) e_{\theta\theta} + (\gamma + 2\mu_T) e_{zz} \end{aligned} \tag{11}$$

Strain and displacement components relations, which are useful in considered study, are as followed:

$$\begin{aligned} e_{rr} &= \frac{\partial u_{SR}}{\partial r}, \\ e_{r\theta} &= \frac{1}{2}\left(\frac{\partial v_{SR}}{\partial r} - \frac{v_{SR}}{r} + \frac{1}{r}\frac{\partial u_{SR}}{\partial \theta}\right), \\ e_{rz} &= \frac{1}{2}\left(\frac{\partial w_{SR}}{\partial r} + \frac{\partial w_{SR}}{\partial z}\right), \\ e_{\theta\theta} &= \frac{1}{r}\left(u_{SR} + \frac{\partial v_{SR}}{\partial \theta}\right), \\ e_{\theta z} &= \frac{1}{2}\left(\frac{1}{r}\frac{\partial w_{SR}}{\partial \theta} + \frac{\partial v_{SR}}{\partial \theta}\right), e_{rz} = \frac{\partial w_{SR}}{\partial z} \end{aligned} \tag{12}$$

where u_{SR}, v_{SR}, and w_{SR} symbolizes the displacement components in r, θ, and z direction respectively.

Together Eq.s (8-12) yield

$$\begin{aligned} r^2\frac{\partial^2 w_{SR}}{\partial r^2} + \frac{\mu_L}{\mu_T}\frac{\partial^2 w_{SR}}{\partial \theta^2} + r\frac{\partial w_{SR}}{\partial r} \\ = r^2\frac{\rho^{SR}}{\mu_T}\frac{\partial^2 w_{SR}}{\partial t^2} \end{aligned} \tag{13}$$

Consider the solution of the equation in harmonic form as

$$w_{SR}(r,\theta,z) = W_{SR}(r)e^{i(n\theta-\omega t)} \tag{14}$$

where W_{SR} is an unknown function.

Solving Eq.s (13) and (14), the obtained equation is

$$\frac{d^2W_{SR}}{dr^2}+\frac{1}{r}\frac{dW_{SR}}{dr}+\left(\frac{\omega^2}{\beta_2^2}-\frac{n^2f^2}{r^2}\right)W_{SR}=0 \tag{15}$$

where $f^2=\frac{\mu_L}{\mu_T}, \beta_2^2=\frac{\mu_L}{\rho^{SR}}$.

Eq. (15) having modified Bessel equation of order nf, whose solution is given by

$$W_{SR} = B_1J_{nf}(\lambda_2 r)+B_2Y_{nf}(\lambda_2 r) \tag{16}$$

where B_1, B_2 are unknown constants, and J_{nf},Y_{nf} are first and second kind Bessel functions respectively.

Substituting Eq. (16) in Eq. (14), which yields the final solution

$$W_{SR} = \left(B_1J_{nf}(\lambda_2 r)+B_2Y_{nf}(\lambda_2 r)\right)e^{i(n\theta-\omega t)} \tag{17}$$

2.3. Boundary Conditions and equations

1. At $r = r_{SR}$
   (a) $T_{rz}^{SR} = 0$
2. At $r = r_{pm}$
   (a) $\psi_{pm} = 0$
   (b) $T_{rz}^{pm} = T_{rz}^{SR}$
   (c) $T_{rz}^{pm} = \alpha_{im}(w_{SR}-u_{pm})$

where α_{im} is a parameter, which represents the interface property, such that $\alpha_{im}\to\infty$ represents the perfectly bonded interface. The dimension of α_{im} is stress/length.

Significance of boundary conditions: the expression of physical laws in differential forms or any form is one of the most fundamental features of theoretical physics, and a discussion of the meaning of this process should always form an important part of the foundation of the topic.

Here the boundary conditions explain that at the outer edge of the figure the boundaries are traction free. At, the interface the stresses are equal following the stress analysis theory.

In the current work, it is assumed that the interface is imperfect mechanically so that the stress component is continuous but the displacement component along the z-direction is discontinuous across the interface.

2.4. Dispersion Relation and equations

Using boundary condition (1) with Eqs. (11), (12), and (17) yields

$$B_1\left(\frac{nf}{\lambda_2 r_{SR}}J_{nf}(\lambda_2 r_{SR})-J_{nf+1}(\lambda_2 r_{SR})\right)+ B_2\left(\frac{nf}{\lambda_2 r_{SR}}Y_{nf}(\lambda_2 r_{SR})-Y_{nf+1}(\lambda_2 r_{SR})\right)=0 \tag{18}$$

Now, using the magnetic potential of Eq. (7) with 2(a) boundary conditions, yields

$$A_2r_{pm}^n + A_1\frac{h_{15}}{\mu_{11}}J_n(\lambda_1 r_{pm}) = 0 \tag{19}$$

Using boundary condition 2(b) with (11), (12), (17), (3), and (7), we have

$$A_2(h_{15}nr_{pm}^{n-1}) = A_1\lambda_1\overline{G}_{pm}\left(-\frac{n}{\lambda_1 r_{pm}}J_n(\lambda_1 r_{pm})-J_{n+1}(\lambda_1 r_{pm})\right) + B_1\left[\mu_T\lambda_2\left(\frac{nf}{\lambda_2 r_{SR}}J_{nf}(\lambda_2 r_{SR})-\right)\right] + B_2\left[\mu_T\lambda_2\left(\frac{nf}{\lambda_2 r_{SR}}Y_{nf}(\lambda_2 r_{SR})-Y_{nf+1}(\lambda_2 r_{SR})\right)\right] \tag{20}$$

Using boundary condition 2(c) with (11), (12), (17), (3), and (7), we have

$$A_2(h_{15}nr_{pm}^{n-1}) = B_1\alpha_{im}J_{nf}(\lambda_2 r_{SR}) + B_2\alpha_{im}Y_{nf}(\lambda_2 r_{SR}) - A_1\left[\lambda_1\overline{G}_{pm}\left(\frac{n}{\lambda_1 r_{pm}}J_n(\lambda_1 r_{pm})-J_{n+1}(\lambda_1 r_{pm})\right)+\alpha_{im}J_n(\lambda_1 r_{pm})\right] \tag{21}$$

For the sake of convenience, the following non-dimensional parameters and variables are considered as

$$\Omega_1 = \lambda_1 r_{pm}, \alpha_1\Omega_1 = \lambda_2 r_{pm}, \beta_1\Omega_1 = \lambda_2 r_{SR},$$

$$\alpha_1=\frac{\lambda_2}{\lambda_1},\qquad \beta_1=\frac{\alpha_1 r_{SR}}{r_{pm}},\qquad \gamma_1=\frac{\alpha_1\mu_T}{\overline{G}_{pm}}, \tag{22}$$

$$k^2=\frac{(h_{15})^2}{\overline{G}_{pm}\mu_{11}},\qquad \Lambda=\frac{\overline{G}_{pm}}{\alpha_{im}r_{pm}}$$

Now, from the Eqs. (22) and (19), Eqs. (18), (20) and (22) results in system of equations involving three arbitrary constantsA_1, B_1andB_2. For nontrivial solutions the determinant of coefficient matrix should vanish, which leads to the dispersion relation for SH-wave propagation in the considered geometry as

$$\begin{vmatrix} f_{11} & f_{12} & f_{13} \\ f_{21} & f_{22} & f_{23} \\ 0 & f_{32} & f_{33} \end{vmatrix} = 0 \tag{23}$$

where

$$f_{11} = \frac{n}{\Omega}(1-k^2)J_n(\Omega) - J_{n+1}(\Omega)$$

$$f_{12} = -\gamma_1\left(\frac{nf}{\alpha_1\Omega}(1-k^2)J_{nf}(\alpha_1\Omega) - J_{nf+1}(\alpha_1\Omega)\right)$$

$$f_{13} = -\gamma_1\left(\frac{nf}{\alpha_1\Omega}(1-k^2)Y_{nf}(\alpha_1\Omega) - Y_{nf+1}(\alpha_1\Omega)\right)$$

$$f_{21} = \{n\Lambda(1-k^2)+1\}J_n(\Omega) - \Omega\Lambda J_{n+1}(\Omega)$$

$$f_{22} = -J_{nf}(\alpha_1\Omega) \qquad (24)$$

$$f_{22} = -Y_{nf}(\alpha_1\Omega)$$

$$f_{32} = \frac{nf}{\beta_1\Omega}J_{nf}(\beta_1\Omega) - J_{nf+1}(\beta_1\Omega)$$

$$f_{33} = \frac{nf}{\beta_1\Omega}Y_{nf}(\beta_1\Omega) - Y_{nf+1}(\beta_1\Omega)$$

3. Numerical results and discussions

Few numerical examples are considered to illustrate the composite material model. The material properties for the PM plate at the surfaces are considered the same as those of the Cobalt Iron Oxide are listed below and for self-reinforcement material also.

Material coefficients for the piezomagnetic layer (Ezzin et al. [13]):

- Chosen Material: $CoFe_2O_4$
- 45.3 G_{pm} $(10^9 N/m^2)$
- 5.3 ρ_{pm} $(10^3 kg/m^3)$
- 157 μ_{11} $(10^{-6} Ns^2/C^2)$
- 550 $h_{15}(N/Am)$

Material coefficients for self-reinforcement material (Singh. B [23]):

- $\mu_L 5.66 \times 10^{10} N/m^2$, μ_T $2.46 \times 10^{10} N/m^2$, ρ^{SR} $2660 kg/m^3$

Figures (2-12) depict the disparity in dimensionless phase velocity of surface wave $(c_d = c/\beta_2)$along with dimensionless wave number $(n_d = nr_{pm})$ for a variety of affecting parameters. Now, in this research article, a study of the dispersion curve is carried out for the first mode of the considered surface wave. Moreover, there is a significant outcome from the present study is that the considered wave phase velocity for the first mode is always decreasing monotonically with a slight increment in the wave number.

Figure 2 depicts the influence of alteration in thickness ratio on the dimensionless phase velocity against the dimensionless wave number. It is noticed that as the width of the overlay increases monotonically keeping the radius of the PM cylinder tube constant, the phase velocity decreases remarkably. Thus, from the result, it is concluded that to optimize the phase velocity of SH surface wave the coating of the self-reinforced layer should be thin. The significant effect of the reinforcement parameter is shown in Fig. 3. For the SH surface wave, the phase velocity rises remarkably with an increment of 0.2 in the considered reinforcement parameter. It is noticeable from figure 3 that the reinforcement affects the phase velocity of SH wave considerably, which governs selecting the exact reinforced material for a thin coating of the MP cylindrical tube to optimize the phase velocity of SH surface wave.

Figures 4 and 5 show the influence of the piezomagnetic coefficient $(\boldsymbol{h_{15}})$ and magnetic permeability$(\boldsymbol{\mu_{11}})$, respectively on the phase velocity of SH surface traveling wave. Observation of these two figures (Figs. 4 and 5) indicates that the higher values of the piezomagnetic coefficient $(\boldsymbol{h_{15}})$ the phase velocity increases whereas the higher values of magnetic permeability$(\boldsymbol{\mu_{11}})$ the phase velocity decreases. So, according to need both types of conditions to occur for increasing and decreasing velocity. Moreover, this vice versa condition of piezomagnetic coefficient $(\boldsymbol{h_{15}})$ and magnetic permeability $(\boldsymbol{\mu_{11}})$ on phase velocity helps to improve the efficiency of magnetic sensors.

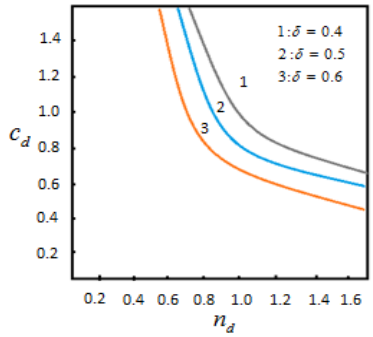

Fig. 2. Variation of dimensionless phase velocity with respect to dimensionless wave number for values to depict the dispersion curves for various values of thickness ratio δ.

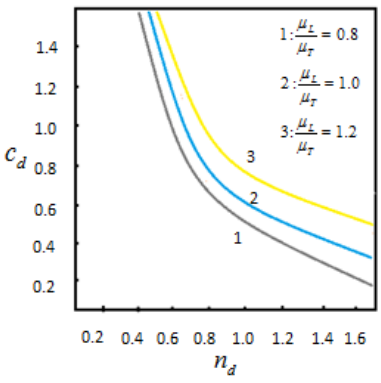

Fig. 3. Variation of dimensionless phase velocity with respect to dimensionless wave number for values to show the dispersion curves for distinct values of reinforcement parameters $\left(\frac{\mu_L}{\mu_T}\right)$.

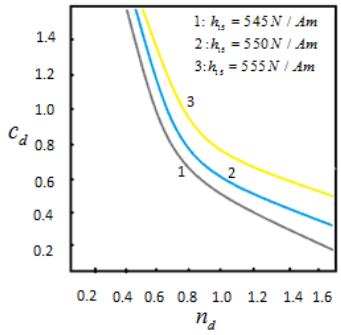

Fig. 4. Variation of dimensionless phase velocity with respect to dimensionless wave number for values to show the dispersion curves for distinct values of piezomagnetic coefficient ($\boldsymbol{h_{15}}$).

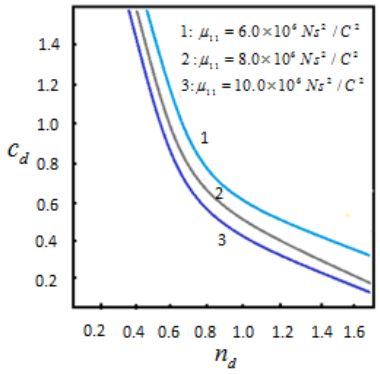

Fig. 5. Variation of dimensionless phase velocity with respect to dimensionless wave number for values to show the dispersion curves for distinct values of magnetic permeability($\boldsymbol{\mu_{11}}$).

Figure 6, governs the influence of initial stress on the phase velocity of SH surface wave. Curve 1 represents the absence of initial stress while curves 2 and 3 are traced out for monotonically increasing values of the radial component of initial stress. From the curves, it is concluded that with the slight increment in the initial stress parameter, the phase velocity increases significantly. The variation in phase velocity against wave number is carved out in Fig. 7 for the presence and absence of imperfection in the interface. In the figure, curve 1 shows the case of perfectly bonded and curve 2 shows the case of the imperfectly bonded interface. It is clearly visible that the phase velocity decreases remarkably in the case of an imperfect interface. This suggests us for optimization of SH-wave phase velocity the bonding of two media (out of which one is PM) should be perfect.

In Fig. 8, it is traced out to depict the dispersion curves for distinct modes of traveling SH surface wave in the considered composite lamina structure. The obtained curves reveal that the dimensionless phase velocity ($\boldsymbol{c_d = c/\beta_2}$) decreases gradually with monotonically increment in the values of the dimensionless wave number ($\boldsymbol{n_d = nr_{pm}}$) for each distinct mode.

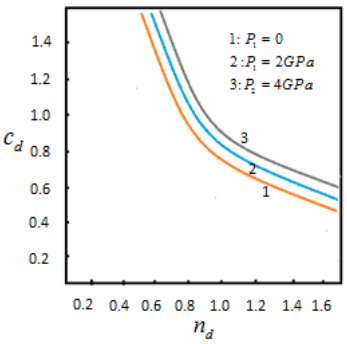

Fig. 6. Variation of dimensionless phase velocity with respect to dimensionless wave number for values to show the dispersion curves for distinct values of the radial component of initial stress ($\boldsymbol{P_1}$)

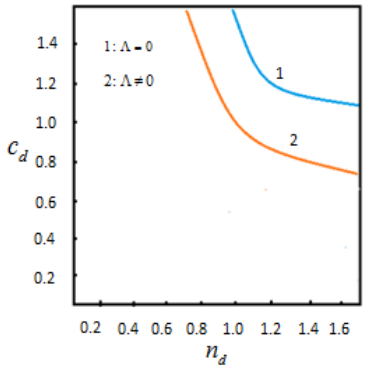

Fig. 7. Variation of dimensionless phase velocity with respect to dimensionless wave number for values to show the dispersion curves for the perfect and imperfect interface.

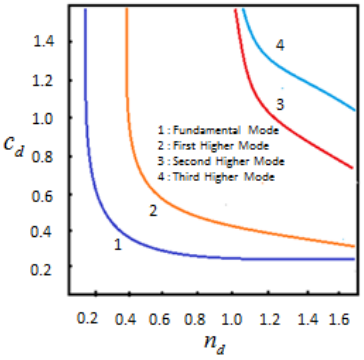

Fig. 8. Variation of dimensionless phase velocity with respect to dimensionless wave number for values to show the dispersion curves for distinct modes.

Moreover, the Figs. 9-11 are developed out to present the influence of mechanical imperfection parameter, reinforcement parameter, and initial stress parameter on phase velocity dispersion curves for regarding higher-order modes. Furthermore, from Fig. 9, it is clearly observed that the surface phase velocity decreases monotonically in presence of mechanical imperfect interface parameters for both second and third modes. Fig. 10 shows that the increment in the value of the initial stress parameter is highly important for the second mode and also, it is significant for the third mode. Fig. 11 delineates the remarkable influence of the

reinforcement parameter on the surface phase velocity for both the second and the third modes. For the considered wave, the surface phase velocity increases monotonically with the gradual increment in the reinforcement parameter. Moreover, Figure 12 represents the dimensionless group velocity (c_g/β_2) against dimensionless wave number (n_d).

Figure 12 shows that the obtained group velocity decreases with the monotonic increase in the wave number. All the figures give valuable information for the choice of PM plate to increase the efficiency of seismic devices and PM sensors.

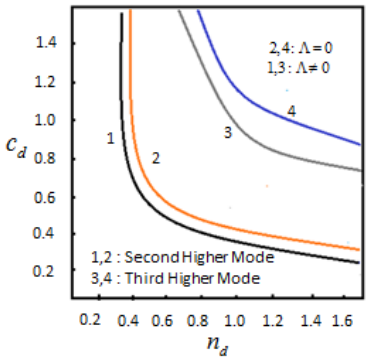

Fig. 9. Variation of dimensionless phase velocity with respect to dimensionless wave number for values to show the dispersion curves for perfect and imperfect interface in higher modes.

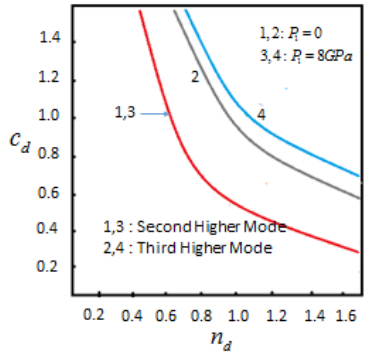

Fig. 10. Variation of dimensionless phase velocity with respect to dimensionless wave number for values to show the dispersion curves for different values of the radial component (P_1) in higher modes.

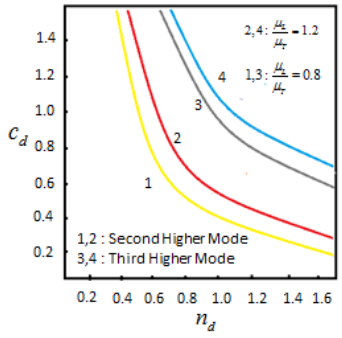

Fig. 11. Variation of dimensionless phase velocity with respect to dimensionless wave number for values to show the dispersion curves for different values of reinforcement parameter $\left(\frac{\mu_L}{\mu_T}\right)$ in higher modes.

Figure 13 depicts the prominent influence of initial stress of considered structure on the phase velocity of surface waves. From Figure 13, it seems that the phase velocity increases when initial stress is present. So, here these results conclude that the wave phase velocity is high in absence of initial stress.

3.1. Significance

One of the sociologically important applications of modern seismology is the monitoring of global underground nuclear testing. The seismic waves generated by such explosions reveal the occurrence of the event as well as provide an estimate of the size of the explosion, mainly by empirical calibration of P- and Rayleigh-wave amplitudes with explosions of known yield, or energy release, in equivalent kilotons of TNT. But first, an event must be identified as an explosion rather than a natural source. Usually, this discrimination of explosion events is accomplished by examining a variety of waveform characteristics that may distinguish earthquakes from explosions. It would seem reasonable to rely mainly on whether or not SH-wave energy is observed, for an explosion source theoretically will not generate significant transverse-component radiation at the source.

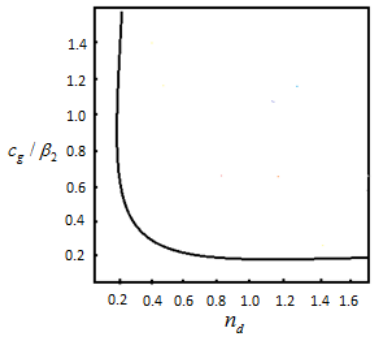

Fig. 12. Variations in dimensionless group velocity (c_g/β_2)against dimensionless wave number (n_d).

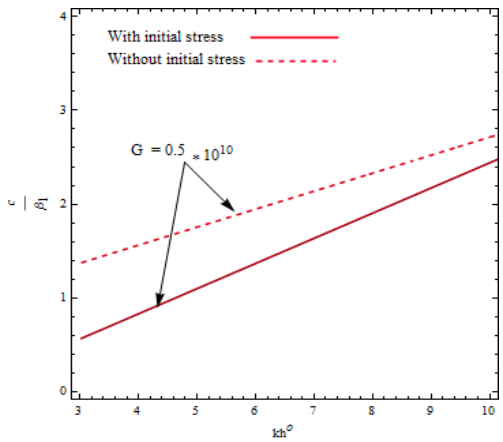

Fig. 13. Variation of dimensionless phase velocity with respect to dimensionless wave number for values of the imperfect parameter with initial stress and without initial stress.

3.2. Validation and equations

When the interface of the two media is perfectly bonded, and the overlay medium is self-reinforced free, then the dispersion relations (23) reduced to

$$\begin{vmatrix} fg_{11} & fg_{g12} & fg_{13} \\ fg_{21} & fg_{22} & fg_{23} \\ 0 & fg_{32} & fg_{33} \end{vmatrix} = 0 \qquad (25)$$

where

$$fg_{11} = \frac{n}{\Omega}(1-k^2)J_n(\Omega) - J_{n+1}(\Omega),$$

$$fg_{12} = -\gamma_1\left(\frac{nf}{\alpha_1\Omega}(1-k^2)J_{nf}(\alpha_1\Omega) - J_{nf+1}(\alpha_1\Omega)\right),$$

$$fg_{13} = -\gamma_1\left(\frac{nf}{\alpha_1\Omega}(1-k^2)Y_{nf}(\alpha_1\Omega) - Y_{nf+1}(\alpha_1\Omega)\right),$$

$$fg_{21} = \{n\Lambda(1-k^2)+1\}J_n(\Omega) - \Omega\Lambda J_{n+1}(\Omega),$$

$$fg_{22} = -J_{nf}(\alpha_1\Omega), fg_{22} = -Y_{nf}(\alpha_1\Omega),$$

$$fg_{32} = \frac{nf}{\beta_1\Omega}J_{nf}(\beta_1\Omega) - J_{nf+1}(\beta_1\Omega),$$

$$fg_{33} = \frac{nf}{\beta_1\Omega}Y_{nf}(\beta_1\Omega) - Y_{nf+1}(\beta_1\Omega), \qquad (26)$$

The obtained dispersion relations are matched with [46].

4. Conclusion

Transference characteristics of horizontally polarized shear wave (SH wave) in a self-reinforced coated piezomagnetic cylinder with a mechanical imperfect bonding interface are studied analytically. The interactions of traveling SH waves with the material properties of adopted composite media/structure give rise to a sensing response. Change in material properties leads to the change in the phase velocity of the wave. The prominent influence of factors affecting the parameters namely mechanical imperfection parameter, reinforcement parameter, thickness ratio, initial stress, piezomagnetic (PM), and magnetic permeability have been studied graphically. More precisely, the following consequences are the crux of meticulous examination of the present study.

- Thinner the coating of a self-reinforced layer higher the phase velocity of SH wave in an adopted composite structure.
- A leap in the value of the reinforcement parameter surmounts the phase velocity. Thus, it is worthy to choose the proper reinforced material to overlay the piezomagnetic cylinder for optimizing the phase velocity of the SH wave.
- Increasing the value of the piezomagnetic constant endorses the phase velocity, while a rise in the value of the dielectric constant diminishes the phase velocity.
- The radial component of the initial stress of the piezomagnetic cylinder shows favoring effect on the phase velocity, as the phase velocity upswings with an increase in the value of initial stress.
- Imperfect bonding of two media scale down the phase velocity. This helps for optimizing the phase velocity of the SH wave the bonding should be perfect.
- In each mode of the propagating SH wave dispersion curve initiates from a certain value, which falls of with increasing value of wave number.

The principle of acoustic wave devices relies on the dispersion characteristics of propagating waves. These devices consist of a multilayer structure. It is apparent from the findings that the imperfect interface of two media reduces the phase velocity remarkably and reinforcement parameter, thickness ratio, initial stress, piezomagnetic and dielectric constants have significant effects on phase velocity. In this view, the outcomes of the study may play an eminent role in designing more efficient acoustic wave devices involving smart materials, especially piezomagnetic cylinders overlaid by a self-reinforced material.

Acknowledgments

The authors convey their sincere thanks to the Department of Computational Sciences, School of Sciences, Christ University for providing all necessary research facilities.

Nomenclature

All variables using this manuscript, listed in nomenclature.

r_{pm}&r_{SR}	Radius of Piezomagnetic and Self-Reinforced Cylinder
δ_{lm}	Kronecker delta
e_{lm}	Strain component
α, β, γ	Elastic constants having dimensions as same as stress
μ_L	Shear modulus in longitudinal direction of reinforcement
μ_T	Shear modulus in transverse direction of reinforcement
Λ	Imperfection Parameter
n	Wave Number
ω	Frequency
c	Phase Velocity

c_g	Group Velocity
μ_L&μ_T	Shear Modulus in longitudinal & in transverse direction
P_1	Radial component of initial stress
J_j&Y_j	Bessel Function of First and Second Kind

References

[1] Ezzin, H., Amor, M.B. and Ghozlen, M.H.B., 2017. Propagation behavior of SH waves in layered piezoelectric/piezomagnetic plates. *Acta Mechanica*, *228*(3), pp.1071-1081.

[2] Kolahchi, R., Hosseini, H. and Esmailpour, M., 2016. Differential cubature and quadrature-Bolotin methods for dynamic stability of embedded piezoelectric nanoplates based on visco-nonlocal-piezoelasticity theories. *Composite Structures*, *157*, pp.174-186.

[3] Nan, C.W., 1994. Magnetoelectric effect in composites of piezoelectric and piezomagnetic phases. *Physical Review B*, *50*(9), p.6082.

[4] Zhao, X., Qian, Z.H., Zhang, S. and Liu, J.X., 2015. Effect of initial stress on propagation behaviors of shear horizontal waves in piezoelectric/piezomagnetic layered cylinders. *Ultrasonics*, *63*, pp.47-53.

[5] Zhou, Y., Chen, W. and Lü, C., 2012. Elastic waves in multiferroic cylinders of sectorial cross-section. *Composites Part B: Engineering*, *43*(8), pp.3001-3008.

[6] Huang, Y., Li, X.F. and Lee, K.Y., 2009. Interfacial shear horizontal (SH) waves propagating in a two-phase piezoelectric/piezomagnetic structure with an imperfect interface. *Philosophical Magazine Letters*, *89*(2), pp.95-103.

[7] Kolahchi, R., 2017. A comparative study on the bending, vibration and buckling of viscoelastic sandwich nano-plates based on different nonlocal theories using DC, HDQ and DQ methods. *Aerospace Science and Technology*, *66*, pp.235-248.

[8] Piliposian, G.T., Avetisyan, A.S. and Ghazaryan, K.B., 2012. Shear wave propagation in periodic phononic/photonic piezoelectric medium. *Wave Motion*, *49*(1), pp.125-134.

[9] Arani, A.G., Kolahchi, R., Barzoki, A.M. and Loghman, A., 2013. The effect of time-dependent creep on electro-thermo-mechanical behaviors of piezoelectric sphere using Mendelson's method. *European Journal of Mechanics-A/Solids*, *37*, pp.318-328.

[10] Sun, W.H., Ju, G.L., Pan, J.W. and Li, Y.D., 2011. Effects of the imperfect interface and piezoelectric/piezomagnetic stiffening on the SH wave in a multiferroic composite. *Ultrasonics*, *51*(7), pp.831-838.

[11] Wang, Y.H., Wang, M.L. and Liu, J.X., 2012. Propagation behaviors of SH waves in piezoelectric layer/elastic cylinder with an imperfect interface. In *Applied Mechanics and Materials* (Vol. 151, pp. 130-134). Trans Tech Publications Ltd.

[12] Li, Y.D., Xiong, T. and Guan, Y., 2016. Effects of coupled interfacial imperfections on SH wave propagation in a layered multiferroic cylinder. *Ultrasonics*, *66*, pp.11-17.

[13] Ezzin, H., Amor, M.B. and Ghozlen, M.H.B., 2016. Love waves propagation in a transversely isotropic piezoelectric layer on a piezomagnetic half-space. *Ultrasonics*, *69*, pp.83-89.

[14] Zhou, Y.Y., Lü, C.F. and Chen, W.Q., 2012. Bulk wave propagation in layered piezomagnetic/piezoelectric plates with initial stresses or interface imperfections. *Composite Structures*, *94*(9), pp.2736-2745.

[15] Abo-el-Nour, N., Al-sheikh, F. and Al-Hossain, A.Y., 2009. Effect of initial stresses on dispersion relation of transverse waves in a piezoelectric layered cylinder. *Materials Science and Engineering: B*, *162*(3), pp.147-154.

[16] Zhao, X., Qian, Z.H., Zhang, S. and Liu, J.X., 2015. Effect of initial stress on propagation behaviors of shear horizontal waves in piezoelectric/piezomagnetic layered cylinders. *Ultrasonics*, *63*, pp.47-53.

[17] Li, Y.D., Xiong, T. and Guan, Y., 2016. Effects of coupled interfacial imperfections on SH wave propagation in a layered multiferroic cylinder. *Ultrasonics*, *66*, pp.11-17.

[18] Guo, X., Wei, P., Li, L. and Lan, M., 2018. Effects of functionally graded interlayers on dispersion relations of shear horizontal waves in layered piezoelectric/ piezomagnetic cylinders. *Applied Mathematical Modelling*, *55*, pp.569-582.

[19] Wu, B., Zhang, C., Chen, W. and Zhang, C., 2015. Surface effects on anti-plane shear waves propagating in magneto-electro-elastic nanoplates. *Smart Materials and Structures*, *24*(9), p.095017.

[20] Sun, C.T. and Cheng, N.C., 1974. Piezoelectric waves on a layered cylinder. *Journal of Applied Physics*, *45*(10), pp.4288-4294.

[21] Dai, H.L. and Wang, X., 2006. Stress wave propagation in piezoelectric fiber reinforced laminated composites subjected to thermal shock. *Composite structures*, *74*(1), pp.51-62.

[22] Spencer, A.J.M., 1972. Deformations of fibre-reinforced materials.

[23] Singh, B., 2006. Wave propagation in thermally conducting linear fibre-reinforced composite materials. *Archive of Applied Mechanics*, *75*(8), pp.513-520.

[24] Belfield, A.J., Rogers, T.G. and Spencer, A.J.M., 1983. Stress in elastic plates reinforced by fibres lying in concentric circles. *Journal of the Mechanics and Physics of Solids*, *31*(1), pp.25-54.

[25] Verma, P.D.S. and Rana, O.H., 1983. Rotation of a circular cylindrical tube reinforced by fibres lying along helices. *Mechanics of Materials*, *2*(4), pp.353-359.

[26] Mahanty, M., Chattopadhyay, A., Dhua, S. and Chatterjee, M., 2017. Propagation of shear waves in homogeneous and inhomogeneous fibre-reinforced media on a cylindrical Earth model. *Applied Mathematical Modelling*, *52*, pp.493-511.

[27] Wang, X., Pan, E. and Roy, A.K., 2007. Scattering of antiplane shear wave by a piezoelectric circular cylinder with an imperfect interface. *Acta mechanica*, *193*(3), pp.177-195.

[28] Fan, H., Yang, J. and Xu, L., 2006. Piezoelectric waves near an imperfectly bonded interface between two half-spaces. *Applied Physics Letters*, *88*(20), p.203509.

[29] Huang, Y., Li, X.F. and Lee, K.Y., 2009. Interfacial shear horizontal (SH) waves propagating in a two-phase piezoelectric/piezomagnetic structure with an imperfect interface. *Philosophical Magazine Letters*, *89*(2), pp.95-103.

[30] Nie, G., Liu, J., Fang, X. and An, Z., 2012. Shear horizontal (SH) waves propagating in piezoelectric–piezomagnetic bilayer system with an imperfect interface. *Acta Mechanica*, *223*(9), pp.1999-2009.

[31] Yuan, L., Du, J., Ma, T. and Wang, J., 2014. Study on SH-SAW in imperfectly bonded piezoelectric structures loaded with viscous liquid. *Acta Mechanica*, *225*(1), pp.1-11.

[32] Chaudhary, S., Sahu, S.A., Singhal, A. and Nirwal, S., 2019. Interfacial imperfection study in pres-stressed rotating multiferroic cylindrical tube with wave vibration analytical approach. *Materials Research Express*, *6*(10), p.105704.

[33] Singhal, A., Sahu, S.A. and Chaudhary, S., 2018. Approximation of surface wave frequency in piezo-composite structure. *Composites Part B: Engineering*, *144*, pp.19-28.

[34] Barati, M.R., 2017. On wave propagation in nanoporous materials. *International Journal of Engineering Science*, *116*, pp.1-11.

[35] Barati, M.R., 2017. On wave propagation in nanoporous materials. *International Journal of Engineering Science*, *116*, pp.1-11.

[36] Zhao, J., Pan, Y. and Zhong, Z., 2012. Theoretical study of shear horizontal wave propagation in periodically layered piezoelectric structure. *Journal of Applied Physics*, *111*(6), p.064906.

[37] Zhao, J., Pan, Y. and Zhong, Z., 2012. Theoretical study of shear horizontal wave propagation in periodically layered piezoelectric structure. *Journal of Applied Physics*, *111*(6), p.064906.

[38] Liu, L., Zhao, J., Pan, Y., Bonello, B. and Zhong, Z., 2014. Theoretical study of SH-wave propagation in periodically-layered piezomagnetic structure. *International Journal of Mechanical Sciences*, *85*, pp.45-54.

[39] Zhao, J., Zhong, Z. and Pan, Y., 2012. Theoretical study of SH-wave propagation in piezoelectric/piezomagnetic layered periodic structures. *The Journal of the Acoustical Society of America*, *131*(4), pp.3327-3327.

[40] Liu, Lei, Yang Yang, Yong-dong Pan, and Zheng Zhong. "The study of wave propagation in the air-coupled composite laminate." *Chinese Journal of Solid Mechanics* 35, no. 1 (2014): 8-14.

[41] Zhang, D., Zhao, J., Bonello, B., Li, L., Wei, J., Pan, Y. and Zhong, Z., 2016. Air-coupled method to investigate the lowest-order antisymmetric Lamb mode in stubbed and air-drilled phononic plates. *AIP Advances*, *6*(8), p.085021.

[42] Sahu, S.A., Mondal, S. and Dewangan, N., 2019. Polarized shear waves in functionally graded piezoelectric material layer sandwiched between corrugated piezomagnetic layer and elastic substrate. *Journal of Sandwich Structures & Materials*, *21*(8), pp.2921-2948.

[43] Kumari, N., Anand Sahu, S., Chattopadhyay, A. and Kumar Singh, A., 2016. Influence of heterogeneity on the propagation behavior of Love-type waves in a layered isotropic structure. *International Journal of Geomechanics*, *16*(2), p.04015062.

[44] Tian, W., Zhong, Z. and Li, Y., 2015. Multilayered piezomagnetic/piezoelectric composites with periodic interfacial cracks subject to in-plane loading. *Smart Materials and Structures*, *25*(1), p.015029.

[45] Hu, K. and Zhong, Z., 2005. A moving mode-III crack in a functionally graded piezoelectric strip. *International Journal of Mechanics and Materials in Design*, *2*(1), pp.61-79.

[46] Belfield, A.J., Rogers, T.G. and Spencer, A.J.M., 1983. Stress in elastic plates reinforced by fibres lying in concentric circles. *Journal of the Mechanics and Physics of Solids*, *31*(1), pp.25-54.